Appendix B

Noise Measurements

A scanning tunneling microscope is extremely sensitive to vibration noise. Changes in the tip-sample separation are exponentially multiplied in the tunneling current: a change in tip-sample separation of as little as an Ångstrom results in an order of magnitude change in the tunneling current. It is therefore extremely important to reduce all external vibrations which might couple to the STM.

This appendix describes the process for measuring the velocity of floor vibrations using a geophone. There is a brief description of electronic noise encountered in geophone measurements, followed by a description of the inner workings of a geophone and a procedure for geophone calibration. Finally, some representative building vibration measurements are reported.

In describing the electronic noise and geophone calibration, I have relied heavily on work done by Eric Hudson and Emile Hoskinson, respectively. I have made some small corrections and clarifications and added a few measurements of my own. It is not my intention to present this document as a body of independent work by myself. However I hope that by bringing the Hudson, Hoskinson, and Hoffman contributions together in one place, this document may serve as a useful reference for future vibration measurements.

B.1 Electronic Noise

Eric Hudson has written a thorough electronic noise summary,[167] and large portions of this section are borrowed from his work. Basic types of electronic noise are:

- **Johnson Noise** arises from fluctuations in voltage across a resistor. Johnson noise takes the form $\Delta V = \sqrt{4k_B T R \Delta f}$. For a resistor at room temperature, Johnson noise becomes $0.13\sqrt{R(\Omega)}$ nV $/\sqrt{\text{Hz}}$.[168] This kind of noise, whose magnitude is flat as a function of frequency, is called "white noise".

- **1/f Noise** arises from fluctuations in the value of the resistance itself, due probably to motion of impurities.[169] This kind of noise, which is the same for each decade of frequency, is called "pink noise".

- **Shot Noise** arises from the quantization of electric charge. At the macroscopic currents we are considering, shot noise will not play a role.

To measure vibrations, one measures the voltage across the two geophone leads. The geophone itself has a resistance r_c, and may also include a damping resistor R_d. The voltage signal is measured using a voltage pre-amplifier and a spectrum analyzer. Choices for the pre-amplifier include: Stanford Research Systems SR560, or Princeton Applied Research 113. Choices for the spectrum analyzer include: Stanford Research Systems SR760 or SR785. Each of these components may contribute electronic noise to the final measurement.

We can measure these sources of noise by working our way up stream from the spectrum analyzer to the pre-amplifier to the geophone. We start by grounding the input to the spectrum analyzer, figuring out the noise of the spectrum analyzer alone, then adding the pre-amplifier, and finally the geophone resistor.

What we are interested in is the "effective input noise". The noise which comes out the final stage of the spectrum analyzer may be quite large, but if we have a very high gain on our pre-amplifier, then our signal is quite large too. The real effect of our output noise must be divided by the gain in order to arrive at the effective input noise.

B.1.1 Spectrum Analyzer

The spectrum analyzer has a front end amplifier stage and an ADC, which each produce noise. After the ADC, everything is digital, so there is no more noise produced after this stage. The noise produced by the ADC does not depend on the spectrum analyzer input gain. Therefore, at high input gain, the effective noise of the ADC is reduced, because the actual noise must be divided by the high gain. Conversely, at low input gain (input attenuation), the effective noise of the ADC is increased. Therefore, we can measure the noise of these two stages independently by setting the input gain to its lowest and highest

levels. At low gains, the ACD noise will dominate, while at high gains, the input amplifier will dominate.

SR760 Spectrum Analyzer

The input gain level ranges from -60dB (i.e. a gain of 1000) to +34dB (i.e. an attenuation of $(1/10)^{(34/20)} = 0.02$). This gain and attenuation occurs in several steps, so the noise may not vary smoothly from one input level to the next, as different gain and attenuation stages are included or excluded.

In fact, as is shown in figures B.1 and B.2, the "noise" of the SR560 is below the level of the lowest ADC bin for most values of the input gain. There remain a few unexplained noise spikes at regular frequency intervals, but these most likely result from the details of the 32-bit logic. All "noise" is below the quoted 90 dB dynamic range of the SR760.

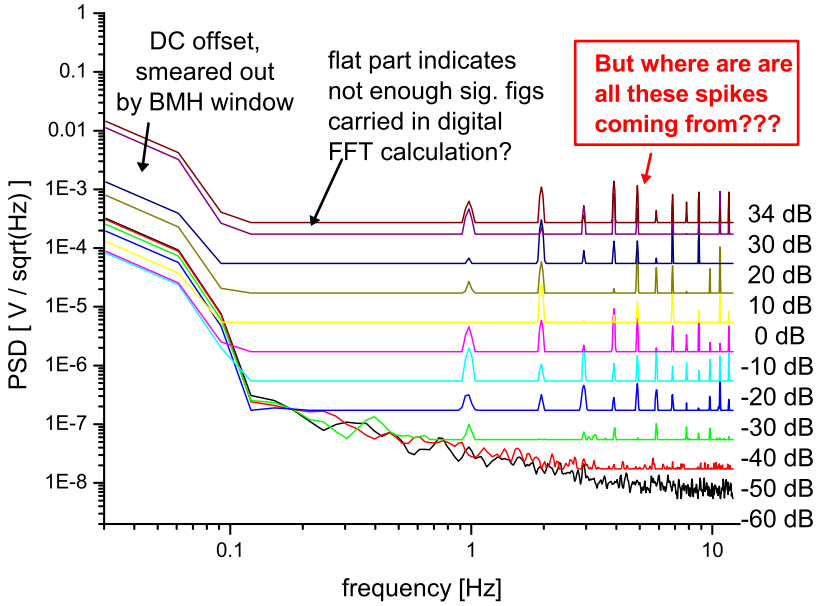

Figure B.1: SR760 noise, characterized in a 12.5 Hz frequency span, for 11 different values of the input level from -34 dB attenuation to 60 dB gain. These spectra show the output of the SR760 with a BNC grounding cap on its input. For the highest values of the input gain, the total noise should be dominated by the input amplifier, while for the lowest values of input gain (i.e. input attenuation), the total noise should be dominated by the ADC. In practice, for all except the highest input gain, the noise is dominated by a series of unexplained spikes superimposed on a constant value which presumably represents the lowest digital bin of the ADC.

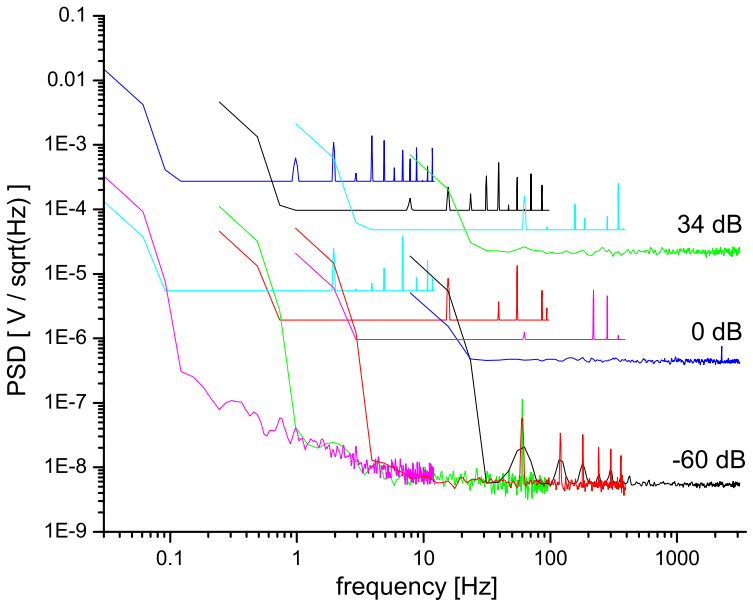

Figure B.2: SR760 noise, characterized across 4 different frequency spans, for 3 different values of the input level from -34 dB attenuation to 60 dB gain. This figure demonstrates that four spectra, all acquired in PSD mode with the same gain, but with different frequency spans, don't match up. The most likely explanation is that they are all in the bottom bit of ADC input, but the digital FFT output is divided by the square-root of the frequency bin size, which is different for each span, to compute the PSD. In order for this explanation to make sense, it must be true that the digital calculations are carried out with more bits than the ADC. In fact, the ADC is 18-bit, with 2 bits reserved for sign, while the digital logic is all carried out with 32 bits.

SR785 Spectrum Analyzer

Both the SR760 and the SR785 have an 18-bit ADC with 2 bits used for sign, so the dynamic range is $2^{16} = 65536$ bins or 90 dB. However the SR785 has a more advanced chip which uses a technique called "noise injection" or "dithering". If the actual signal is relatively quiet, and sits, say 80% of the way between bins 1 & 2, then the ADC will always convert the signal into bin 2. However, if the input signal contains some noise of amplitude larger than the bin width, and if the ADC samples the input multiple times, then it can actually measure a value to much greater accuracy than the bin size. Of course this is only relevant if the internal digital calculations are carried out with greater bit resolution than the nominal bit resolution of the ADC. In the case of the SR785, the input ADC is 18-bit (with 2 bits reserved for sign) with input dithering, while the digital logic is carried out with 32 bits, so the effective dynamic range is much larger than the quoted 90 dB.

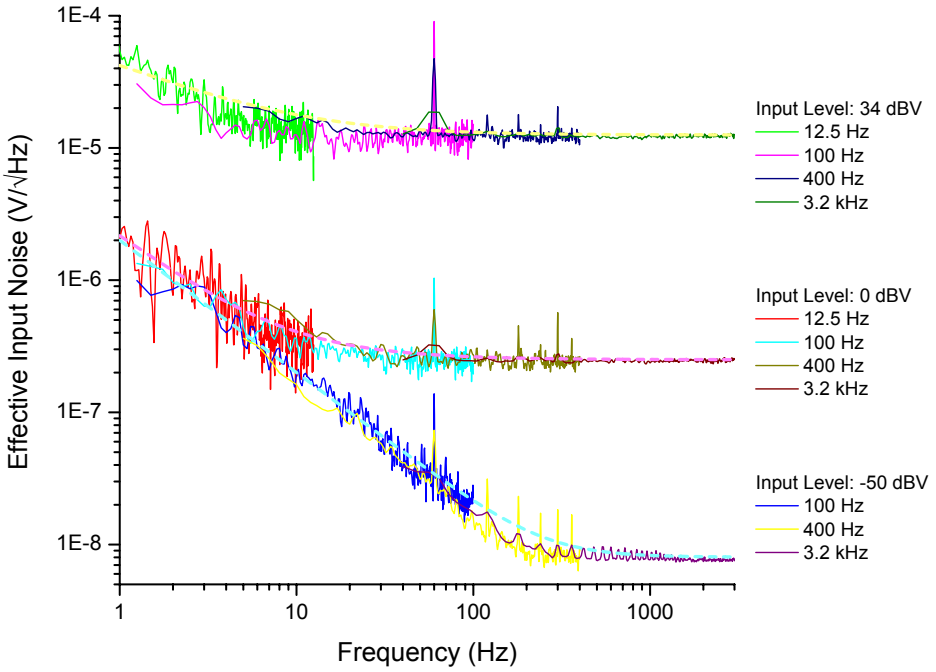

Figure B.3: SR785 noise characterization, by Hudson.[167] Measurements were taken with the SR785 input grounded, at 3 different ranges, for 4 different frequency spans.

The input stage of the SR785, as characterized by Hudson[167], has a $1/f$ noise of $\sim 2f^{-1}$ $\mu\text{V}/\sqrt{\text{Hz}}$ and a high frequency noise floor of 8 $\text{nV}/\sqrt{\text{Hz}}$. The signal then passes through a gain depending on the input level setting (IL in dBV): gain $= 10^{(-IL/20)}$. The input level ranges from -50 dbV to 34 dbV in 2 dbV steps. The ADC has a $1/f$ noise of ~ 0.8 $\mu\text{V}/\sqrt{\text{Hz}}$ and a high frequency noise floor of ~ 250 $\text{nV}/\sqrt{\text{Hz}}$.

FFT Windowing

Another effect to consider is FFT windowing. The spectrum analyzer captures a time sequence of voltage samples. But the FFT algorithm assumes that this sequence will be periodic, i.e. that the first point will match up to the last point.[170] Of course this is not generally the case for actual measurements of an arbitrary time sample, so there will be a sharp step in the voltage at the boundary between the beginning and the looped around end. This sharp step has high frequency components, higher than the Nyquist frequency of 1/2 the sampling rate. So these high frequency components will be folded back and create inaccuracies in the output FFT.

The way to ameliorate (but not completely fix) this problem is to apply a windowing

function to the captured time sequence, which sends the beginning and the end smoothly to zero. None of these windows are perfect, and there will always be some leakage from one frequency bin to the next. This is perhaps most relevant at very low frequencies. The input stage of the spectrum analyzer has some DC offset. Although the spectrum analyzer automatically self calibrates every half hour or so, it will always have some DC offset. In practice, this offset seems to be is larger than the signals we are trying to measure at any other frequency. Because of windowing, the DC offset becomes spread out across several adjacent low-frequency bins, as can be seen in figure B.1.

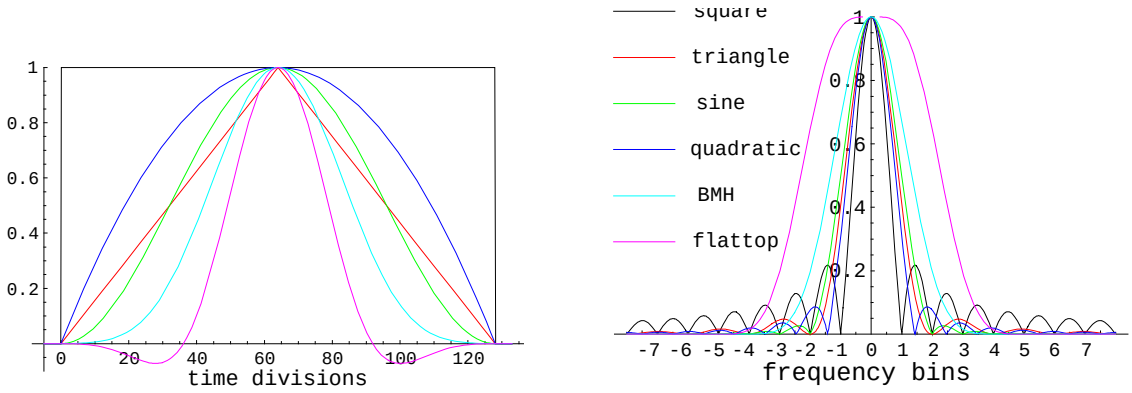

(a) (b)

Figure B.4: Fourier transform windowing functions. (a) Real space windowing functions: all go smoothly to zero at the beginning and end of the time trace except for the square window. (b) Frequency effect of windowing functions: leakage to adjacent frequency bins.

By judicious choice of a windowing function we can minimize the number of adjacent bins into which the DC offset signal will spill. A typical choice (recommended in the spectrum analyzer manual) is the BMH window. Also, by taking measurements across lower and lower frequency ranges (i.e. more and more time consuming measurements) we can push down the frequency at which the DC offset will plague us.

B.1.2 Voltage Pre-Amplifier

SR560 Voltage Pre-Amplifier

The noise floor of the SR560 consists of two main components: a high frequency white noise floor that depends on the gain and dynamic reserve setting, and a $1/f$ component. At the highest gain and low noise setting, the minimum white noise is just less than 4 $\mathrm{nV}/\sqrt{\mathrm{Hz}}$. The white noise for all values of the SR560 gain is summarized in table B.1. The

$1/f$ noise prefactor appears to scale linearly with the white noise for each gain; the constant of proportionality is ~ 4.5.

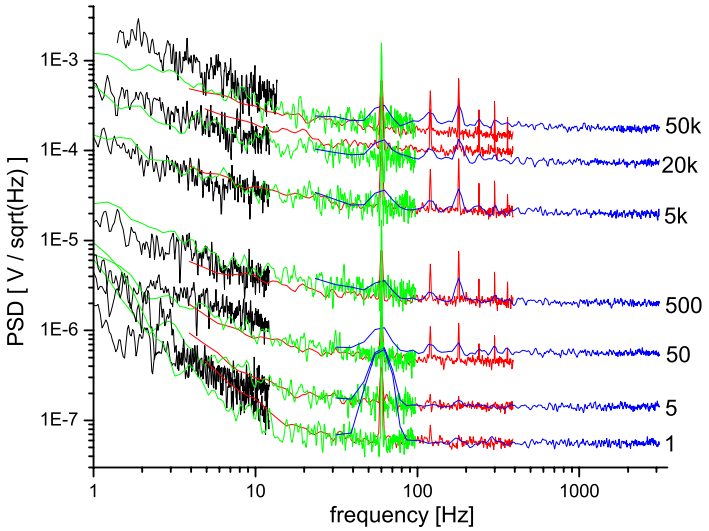

Figure B.5: SR560 noise characterization for seven different values of the SR560 gain, from 1 to 50,000. Measurements were taken with the SR560 input grounded, and the SR560 output connected to the input of the SR760.

Gain	eff. input noise [nV/$\sqrt{\text{Hz}}$]
1	56.9
2	38.4
5	29.2
10	13.3
20	12.0
50	9.0
100	4.3
200	4.1
500	4.1
1,000	4.1
2,000	4.0
5,000	3.9
10,000	3.9
20,000	3.7
50,000	3.6

Table B.1: SR560 effective input noise characterization, measured for all values of the SR560 gain from 1 to 50,000.

PAR 113 Voltage Pre-Amplifier

At the highest gain of the PAR 113, the minimum white noise is $\sim$ 1-2 nV/$\sqrt{\text{Hz}}$, significantly better than the SR560.

B.1.3 Geophone

The resistor(s) in the geophone r_c (and R_d if applicable), each contribute Johnson noise. Our source resistance for the largest geophone used was $r_c = 4500\ \Omega$, and for the smaller geophones used more frequently is typically $r_c = 500\ \Omega$. Therefore, using the Johnson noise formula $0.13\sqrt{R(\Omega)}$ nV /$\sqrt{\text{Hz}}$, the large and small geophones will contribute 8.7 and 2.9 nV /$\sqrt{\text{Hz}}$, respectively.

The geophone resistors will also contribute a $1/f$ noise component. However, this $1/f$ noise will be very difficult to separate from a true vibration signal.

B.1.4 Total Electronic Noise

Taking all noise sources together, the combined effective input noise from the geophone r_c, the SR560, and the SR785, is given by:

Effective input noise (nV / $\sqrt{\text{Hz}}$)

$$= \frac{\sqrt{\left(\left(\text{PreampOutputNoise}^2 + \left(\frac{2000}{f}\right)^2 + 8^2\right) \times 10^{(-IL/20)} + \left(\frac{800}{f}\right)^2 + 250^2\right)}}{10^{(-IL/20)} \times \text{PreampGain}} \quad \text{(B.1)}$$

$$= \sqrt{\text{PreampInputNoise}^2 + \frac{\left(\frac{2000}{f}\right)^2 + 8^2 + \left(\left(\frac{800}{f}\right)^2 + 250^2\right) \times 10^{(IL/20)}}{\text{PreampGain}^2}} \quad \text{(B.2)}$$

where PreampInputNoise is the geophone noise plus the effective input noise of the pre-amplifier itself, and IL is the input level of the SR785. Equation B.2 makes clear that to minimize noise we want to use as large a pre-amplifier gain as possible (since the input noise is fixed by the source impedance and the amplifier specifications) and as small an input level as possible (to minimize effects of ADC noise).

To find the noise floor of the vibration measurements in real velocity units, we would just divide this by the (frequency dependent) sensitivity of the geophone.

B.2 How a Geophone Works

Large portions of the section are borrowed from Emile Hoskinson's geophone calibration report.[171] My modifications include:

- fixed a few errors in formulas
- additional figures & circuit diagrams
- equations to calibrate a geophone which has a permanent series resistor R_d

There are two common ways to make vibration measurements. One is intrinsically a velocity-measurement device, while the other is intrinsically an accelerometer.

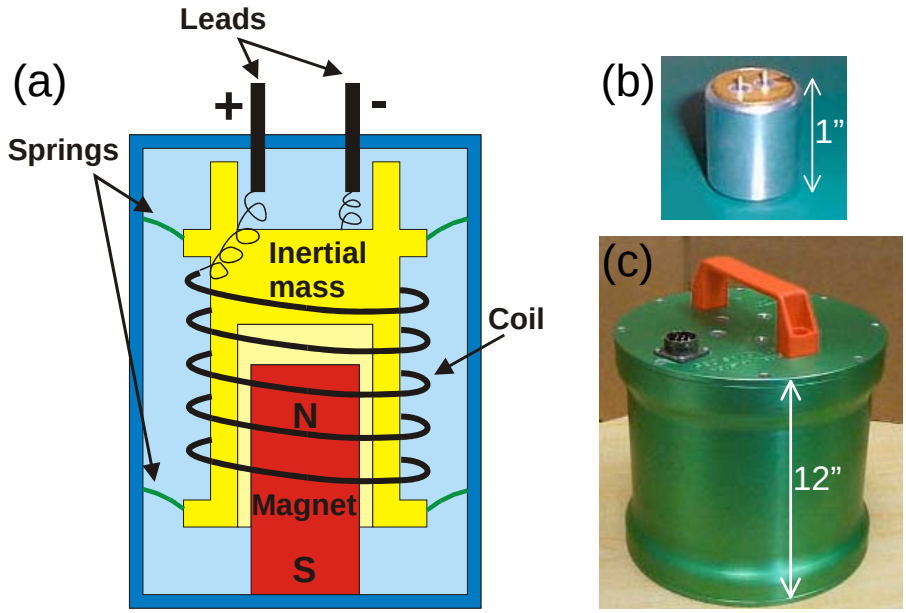

Figure B.6: (a) Schematic of a typical geophone. A massive coil on springs moves with respect to a fixed magnet, inducing a current in the coil which can then be read out as a voltage across the geophone resistance. (b) Photo of a small HS-J geophone from GeospaceLP. (c) Photo of a monstrous green 3-axis geophone, which contains 3 separate GS-1 geophones.

Typically, velocity is measured with a geophone, which consists of a massive coil on a spring, which can move with respect to a fixed magnet. The motion of the coil with respect

to the magnet induces an *emf* in the coil, which can then be put in series with a resistor to produce a measurable voltage. A diagram of a geophone is shown in Fig. B.6.

When the case of the geophone accelerates, the coil moves relative to the fixed magnet, and induces a voltage across the coil:

$$V = -N\frac{d\Phi}{dt} = -N\frac{d\Phi}{dx}\dot{x} \tag{B.3}$$

where N is the number of coil turns, and Φ is the magnetic flux produced by the permanent magnet. We see that the voltage produced is proportional to the velocity, therefore the geophone is intrinsically a velocity-measuring device, with sensitivity G defined by: $V \equiv G\dot{x}$. We can read off the sensitivity from Eq. B.3 as:

$$G = -N\frac{d\Phi}{dx} \tag{B.4}$$

Let's give some thought to the direction of winding of the coil. In the center of the coil, $d\Phi/dx < 0$ by geometry. If the coil moves up with respect to the fixed magnet, then $\dot{x} > 0$, and $d\Phi/dt < 0$. Lens' law requires that the induced current oppose the decrease in upwards pointing flux, so the induced current must create a flux Φ_{ind} which points up, so the induced current must be counter-clockwise. We define the direction of positive current flow to be from the plus terminal to the minus terminal, down around the coil, or counter-clockwise as viewed from above. Therefore an upwards motion of the coil with respect to the fixed magnet produces a positive current and a positive voltage across the terminals from plus to minus. This means that $G > 0$, as we would hope.

If the geophone leads are unconnected, no current flows and the only damping is mechanical, described by a damping constant D. If the geophone drives an external resistive load R_d, then a current I flows through the geophone:

$$V \equiv G\dot{x} = I(R_d + r_c) - L\frac{dI}{dt} \tag{B.5}$$

where r_c is the coil resistance and L is the coil inductance. For an excitation at frequency ω, $\dot{I}(t) \approx \omega I$, so the inductive term will be negligible if $\omega L/(R_d + r_c) \ll 1$.

For example, the values from some GeospaceLP geophones are: [a]

[a] http://www.geospaceLP.com

geophone	$r[\Omega]$	$L[H]$	L/r	$\omega L/r$ $[f = 10$ Hz$]$	$\omega L/(R+r)$ $[f = 100$ Hz$]$ $[R = 10r]$
HS-1 (V)	208	0.029	1.40×10^{-4}	0.009	0.008
HS-J-L1 (H1)	1232	0.327	2.65×10^{-4}	0.016	0.015
HS-J-L1 (H2)	306	0.079	2.58×10^{-4}	0.017	0.015
GS-1 (V)	4613	1.440	3.12×10^{-4}	0.020	0.018
GS-1 (H1)	4557	1.903	4.18×10^{-4}	0.026	0.024
GS-1 (H2)	4555	1.982	4.35×10^{-4}	0.027	0.025

Therefore, we can safely ignore the voltage contribution from the inductance of the coil for frequencies below $f \approx 10$ Hz with no damping resistor R, and for frequencies below $f \approx 100$ Hz with a damping resistor $R = 10r$. Neglecting the inductance, we see that the current is proportional to the velocity:

$$I = \frac{G}{R+r}\dot{x} \tag{B.6}$$

There is an additional force on the mass when a current flows, due to the force of the fixed magnetic field gradient which acts on the coil (approximated as a dipole of area NA, where N is the number of loops and A is the area of a single loop).

$$F = m\nabla B = NIA\frac{dB}{dx} = N\frac{d\Phi}{dx}I = -GI = -\frac{G^2}{R_d + r_c}\dot{x} \tag{B.7}$$

For a $\dot{x} > 0$, the current is positive, and the dipole $m = NIA$ points up, while the gradient in field points down, so the resultant force on the coil is down, opposing the direction of motion. Therefore, the flow of current acts as an additional damping force with damping coefficient $G^2/(R+r)$ so the total damping coefficient is now:

$$d = D + \frac{G^2}{R_d + r_c} \tag{B.8}$$

We can compare the strength of the two damping forces. Some approximate parameters are (for an external resistor $R = 0$, short circuit):

geophone	D	G [V/(m/s)]	$r[\Omega]$	G^2/r
HS-J-L1 (V)	11.0	30	1250	26.5
HS-J-L1 (H1)	6.6	15	300	38.4
GS-1 (V)	0.15	350	4600	0.74
GS-1 (H1)	0.23	420	4550	1.14

Therefore, we see that the electromagnetic damping is much larger than the mechanical damping, so it is important to short the geophone when moving it, to electromagnetically clamp the mass in place an avoid damage to the springs due to the fatigue from violent stretching and compressing.

Taking into account both sources of damping, the sum of all the forces on the mass is therefore:

$$m\ddot{x} = -GI - D\dot{x} - kx \tag{B.9}$$

B.3 Geophone Calibration

A nice, easy-to-automate way to calibrate the geophone (thanks to Emile Hoskinson[171]) is to put a resistor in series with the geophone, apply a sine wave voltage of variable frequency, and map the response voltage across the geophone as a function of frequency. The circuit diagram is shown in Fig. B.7.

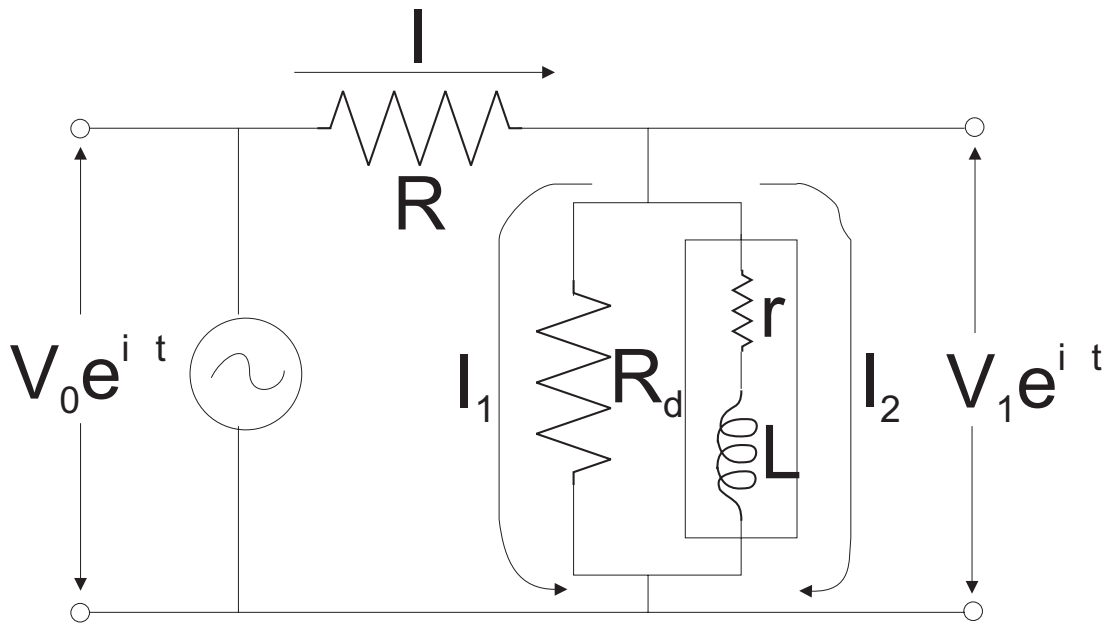

Figure B.7: Circuit diagram for automated geophone calibration.

For full generality, we have included a parallel damping resistor R_d in addition to the series resistor R, because some Geospace geophones such as the GS-1's come with a permanent damping resistor which can't be removed. (In the smaller geospace geophones such as

the HS-J-L1's, there is no damping resistor, so we can take $R_d \to \infty$.) In the configuration of Fig.B.7, the sum of all the voltages around the loop is:

$$V_0 e^{i\omega t} + G\dot{x} = IR + I_2 r \tag{B.10}$$

where we have equated the sources of *emf* on the left side with the resultant voltages across the components on the right side (again ignoring the contribution from the inductor, which we already argued was negligible.)

The voltage across the geophone plus series resistor is therefore:

$$V_0 e^{i\omega t} = IR + I_2 r - G\dot{x} \tag{B.11}$$

while the voltage across the geophone alone is:

$$V_1 e^{i\omega t} = V_0 e^{i\omega t} - IR = I_2 r - G\dot{x} \tag{B.12}$$

We can measure the magnitude and phase of V_1/V_0 as a function of frequency, fit each to a pre-calculated functional form, and therefore have two independent measurements of the important parameters of the geophone.

So let's calculate the expected functional form of V_1/V_0. To do this, we first eliminate the currents I and I_2 from the ratio. We note that:

$$I = I_1 + I_2; \quad I_1 R_d = I_2 r \qquad \Rightarrow \qquad I = I_2 \left(1 + \frac{r}{R_d}\right) \tag{B.13}$$

We can find I_2 from the modified version of Eq. B.9:

$$m\ddot{x} = -GI_2 - D\dot{x} - kx \tag{B.14}$$

where the only difference is that now the current flowing through the geophone coil (which is responsible for the damping) is called I_2 instead of I.

This can be re-written as:

$$\ddot{x} + 2\alpha_0\omega_0\dot{x} + \frac{G}{m}I_2 + \omega_0^2 x = 0 \tag{B.15}$$

where $\omega_0 \equiv \sqrt{k/m}$ is the mechanical resonance frequency, and $\alpha_0 \equiv D/(2m\omega_0)$ is the mechanical damping as a fraction of critical damping.

Now we let $\dot{x} = v_0 e^{i\omega t}$, where v_0 may be complex. We can substitute this into Eq. B.15, and solve for I_2:

$$I_2 = -\left[D + im\omega\left(1 - \frac{\omega_0^2}{\omega^2}\right)\right]\frac{v_0 e^{i\omega t}}{G} \tag{B.16}$$

Now we can substitute Eqs. B.13 and B.16 into Eqs. B.11 and B.12, and after some messy algebra, we arrive at:

$$\frac{V_1}{V_0} = \frac{I_2 r - G\dot{x}}{IR + I_2 r - G\dot{x}} = c + \frac{2sc(1-c)}{2\alpha_0 + 2sc + iz} \tag{B.17}$$

where we have defined the following (real) constants:

$$c \equiv \frac{rR_d}{rR_d + RR_d + rR}; \qquad s \equiv \frac{G^2}{2m\omega_0 r}; \qquad z \equiv \frac{\omega}{\omega_0}\left(1 - \frac{\omega_0^2}{\omega^2}\right) \tag{B.18}$$

Note that c is just the ratio V_1/V_0 at DC. In the case of no damping resistor, $R_d \to \infty$ and $c \to r/(r+R)$.

After some more messy algebra, we can arrive at expressions for the magnitude and phase of the ratio:

$$\left|\frac{V_1}{V_0}\right| = c\sqrt{1 + \frac{4b[2\alpha_1 + b]}{4\alpha_1^2 + z^2}} \tag{B.19}$$

$$\theta = \arctan\frac{\mathrm{Im}(V_1/V_0)}{\mathrm{Re}(V_1/V_0)} = \arctan\left(\frac{-z}{2\alpha_1 + \frac{1}{2b}(4\alpha_1^2 + z^2)}\right) \tag{B.20}$$

where we have defined the additional constants:

$$\alpha_1 \equiv \alpha_0 + sc; \qquad b = s(1-c) \tag{B.21}$$

Now we use a Labview program (primarily written by Emile Hoskinson) to sweep the frequency and measure the response, and we can independently do a three parameter fit (α_1, b, and ω_0) to the magnitude and phase of the response to determine the three physical

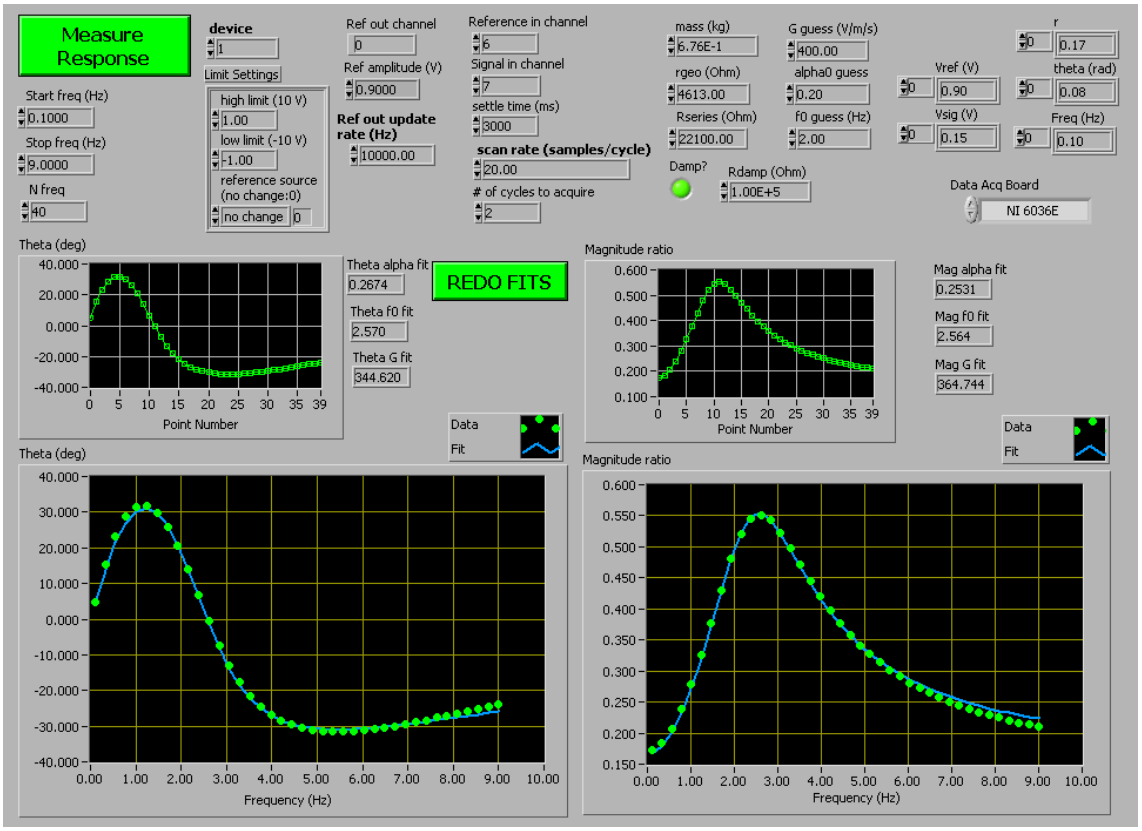

Figure B.8: Labview output for geophone calibration. The graph on the lower left shows the fit to the phase of V_1/V_0 while the graph on the lower right shows the fit to the magnitude of V_1/V_0.

parameters resonance frequency (f_0 via ω_0), sensitivity (G via b and α_1) and damping (α_0 via b and α_1). A typical output is shown in figure B.8.

So now we know f_0, α_0, and G, how do we use them to turn our geophone's output voltage into a velocity in real world units? The full system is described by the differential equation:

$$m(\ddot{x} + \ddot{w}) + d\dot{x} + kx = 0 \tag{B.22}$$

where $x(t)$ is the displacement of the coil relative to the case, $\ddot{w}(t)$ is the acceleration of the case (fixed to the ground), and d is the total damping constant ($d = D$ in case of no damping resistor, while $d = D + G^2/(r + R_d)$ for damping resistor R_d). This can be rewritten as:

$$\ddot{x} + 2\alpha\omega_0\dot{x} + \omega_0^2 x = a_g e^{i\omega t} \tag{B.23}$$

where α is now the total damping constant as a fraction of critical damping, and we have taken the acceleration of the case with respect to the ground for a fixed frequency to be $a_g e^{i\omega t}$.

This equation can be solved by substituting $x = x_c e^{i\omega t}$. We solve for x_c (the position of the coil relative to the case) in terms of a_g (the acceleration of the ground):

$$x_c = \frac{a_g}{(\omega^2 - \omega_0^2) - 2i\alpha\omega_0\omega} \tag{B.24}$$

But we know that the *emf* produced by the geophone will be proportional to the velocity (and we don't care about phase, just maximum amplitude, so we take $|v_c| = |\omega x_c|$ and $|a_g| = |\omega v_g|$), so we can write:

$$\begin{aligned} |V| &= |Gv_c| = \left| \frac{G\omega^2 v_g}{(\omega^2 - \omega_0^2) - 2i\alpha\omega_0\omega} \right| \\ &= \frac{G\left(\frac{\omega^2}{\omega_0^2}\right) v_g}{\sqrt{\left(1 - \frac{\omega^2}{\omega_0^2}\right)^2 + 4\alpha^2 \frac{\omega^2}{\omega_0^2}}} \end{aligned} \tag{B.25}$$

There is one remaining complication: Eq. B.25 gives the total *emf* produced by the geophone coil, but this *emf* causes a current to flow through r and possibly R_d (if there is an R_d). We assume for the purposes of measurement that we are using a pre-amplifier with effectively infinite input impedance, so $R \to \infty$ and no current flows except around the loop through r and R_d. Therefore the *emf* is split between the two resistors, and our measured voltage is multiplied by a factor of $R_d/(R_d + r)$ (which of course reduces to 1 in the case where there is no damping resistor R_d).

Therefore, our velocity in real world units is:

$$v_g = V_{\text{meas}} \div \left\{ \frac{G\left(\frac{f^2}{f_0^2}\right)\left(\frac{R_d}{R_d+r}\right)}{\sqrt{\left(1 - \frac{f^2}{f_0^2}\right)^2 + 4\alpha^2 \frac{f^2}{f_0^2}}} \right\} \tag{B.26}$$

where we must calculate α from α_0 according to the value of R_d:

$$\alpha = \frac{1}{2m\omega_0}\left(D + \frac{G^2}{R_d + r}\right) \tag{B.27}$$

B.3.1 Geospace Parameters

In the calibration procedure described above, the only parameter we need to use which we can't measure directly is the mass of the coil. We just need to take Geospace's word for this one. We can measure the resistances ourselves with an ohm-meter.

But it's useful to put in reasonable initial guesses for the various parameters of our fit. And it's nice to be able to compare our final calibration results with the company specs. So here is a list of parameters typically given by Geospace, and what they mean:

Parameter	Geospace Symbol	Our Symbol
Natural Frequency	F_n	f_0
Suspended Mass	m	m
Coil Resistance	R_C	r
Coil Inductance	L_C	L
Damping Resistor	R_L	R_d
Sensitivity		G
Open Circuit Damping	B_0	α_0
Damping Constant	B_C	
Shock		
Coil/Case Displacement Limit		
Overswing (A1)		
Overswing (A2)		

Of these parameters, we have discussed all but the last five. Shock is the maximum shock sustainable by the geophone without damage (presumably this means with the geophone leads shorted, although it doesn't say so explicitly). For example, the maximum shock for the GS-1 geophones (the ones inside the big green cylinder) is $50g$ which is approximately equivalent to dropping the geophone from a height of 5 cm onto a tile floor which will deform by 1 mm on impact.

The coil/case displacement limit is irrelevant to us.

The overswings A1 & A2 are related to an alternate calibration method involving the measurement of subsequent transient response peaks.[171] A1 & A2 are the magnitudes of the first two transient response peaks, apparently in terms of oscilloscope divisions as measured at Geospace.

The damping constant B_c is redundant information with the open circuit damping B_0.

It is used for an easy determination of the damping resistance R_d the user must add to achieve a given total damping α. Geospace gives the formula as:

$$R_L = \frac{B_C}{B_T - B_0} - R_C \tag{B.28}$$

or, in our language:

$$B_C = (\alpha - \alpha_0)(R_d + r) \tag{B.29}$$

Comparing this to equation B.8 and recalling that $\alpha = d/(2m\omega_0)$ we see that:

$$B_C = \frac{G^2}{2m\omega_0} \tag{B.30}$$

If we do this calculation for multiple geophones and compare our calculated B_C from Geospace's reported B_C, we find that we are consistently off by a factor of 159, which must be some strange way that Geospace is reporting their units.

B.4 Vibration Results

The STM used in this thesis was located in the basement of Birge Hall at the University of California, Berkeley. The room actually protruded underground from the main footprint of the building, and was surrounded by dirt on five sides. This resulted in an extremely quiet environment. However, even in this isolated "bunker", external events would occasionally couple vibrations into the STM. In rare cases, external vibrations were responsible for crashing the STM tip into the sample, which invariably ended the data run and forced a time consuming temperature cycle. Therefore, we conclude that the vibration profile surrounding this STM defines an approximate cutoff for an acceptable STM operating environment.

I have compiled vibration data from several STM labs around the United States (thanks to Don Eigler for data from IBM Almaden, Séamus Davis for data from Cornell University, Eric Hudson for data from NIST Gaithersburg and MIT, and Ali Yazdani for data from the University of Illinois Urbana-Champaign). The comparison of the data from these STM labs is show in figure B.9.

Vibrations from five of the labs lie within an order of magnitude of each other, with

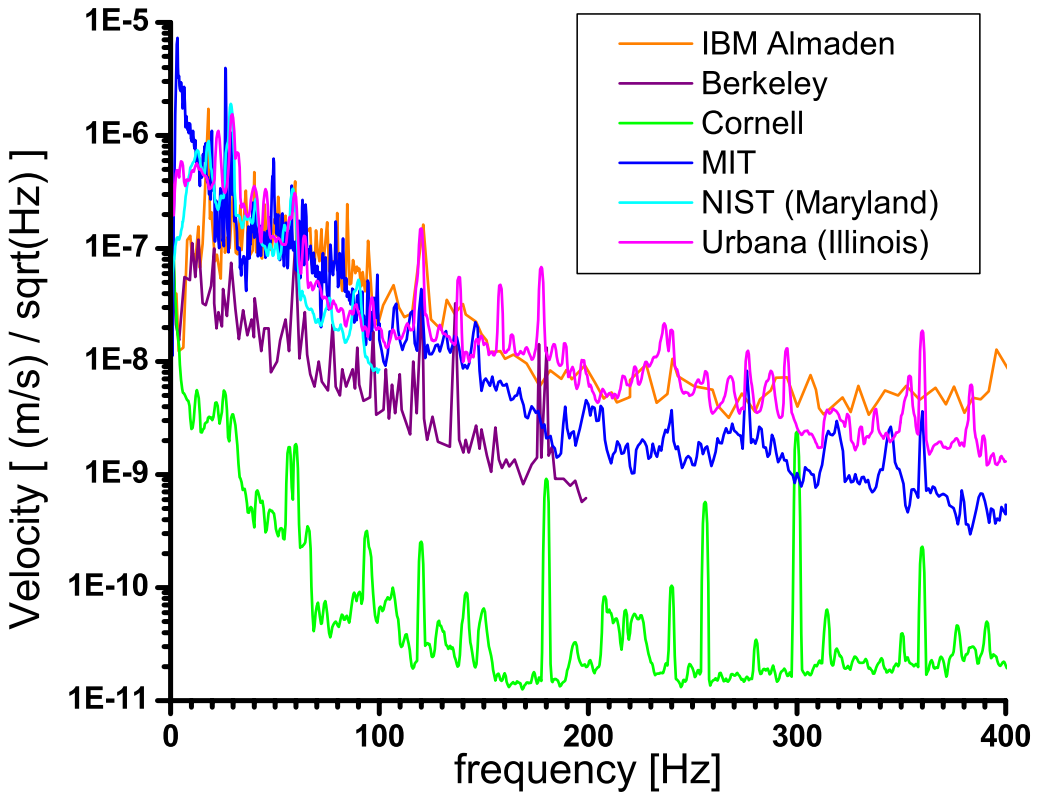

Figure B.9: Vibration measurement results from several STM labs around the country.

Berkeley showing the best performance of the five. Conspicuously several orders of magnitude quieter than Berkeley are the new ultra-low-vibration labs constructed by Séamus Davis at Cornell University. These labs consist of 30-ton slabs of concrete, floating on air spring isolators. The entire experiment is enclosed in a double-walled sound room, with the outer wall of cinder blocks and sand, and the inner wall a commercial mineral rock product from IAC. Although the steady-state vibration levels in these labs are perhaps overkill for STM, the major advantage is complete freedom from the isolated very noisy events which can crash an STM tip and destroy 3 months of work.

1/3-Octave analysis

We physicists prefer to display vibration data as a narrow band spectrum in $(\mathrm{m/s})/\sqrt{\mathrm{Hz}}$, because it conveys the largest amount of data. However, the architectural standard for talking about vibrations is 1/3-octave analysis. This is essentially a smoothing technique, which integrates noise over frequency ranges whose widths are proportional to their center

frequencies. Specifically, we display the total integrated rms noise in a band centered at f_0 with width $2^{1/3} \times f_0$. A 1/3-octave band spectrum can easily be calculated from a narrow-band spectrum by adding up the appropriate bins.

American architects also like to talk in μinches/s rather than m/s. They have defined a set of vibration criteria, labeled VC-A through VC-E, where B is twice as quiet as A, C is twice as quiet as B, etc. In order to meet a specific vibration criterion, a room's vibrations must lie entirely below the relevant VC line at at all frequencies. It turns out that the minimum acceptable vibration criterion for STM lies well below the most stringent criterion acknowledged by architectural standards, VC-E. In fact, if we extend the vibration criteria lettering scheme using the same factor of 2 relations, we find that Séamus Davis' new Cornell labs would satisfy VC-M! The same data from figure B.9 are replotted in the architectural units in figure B.10.

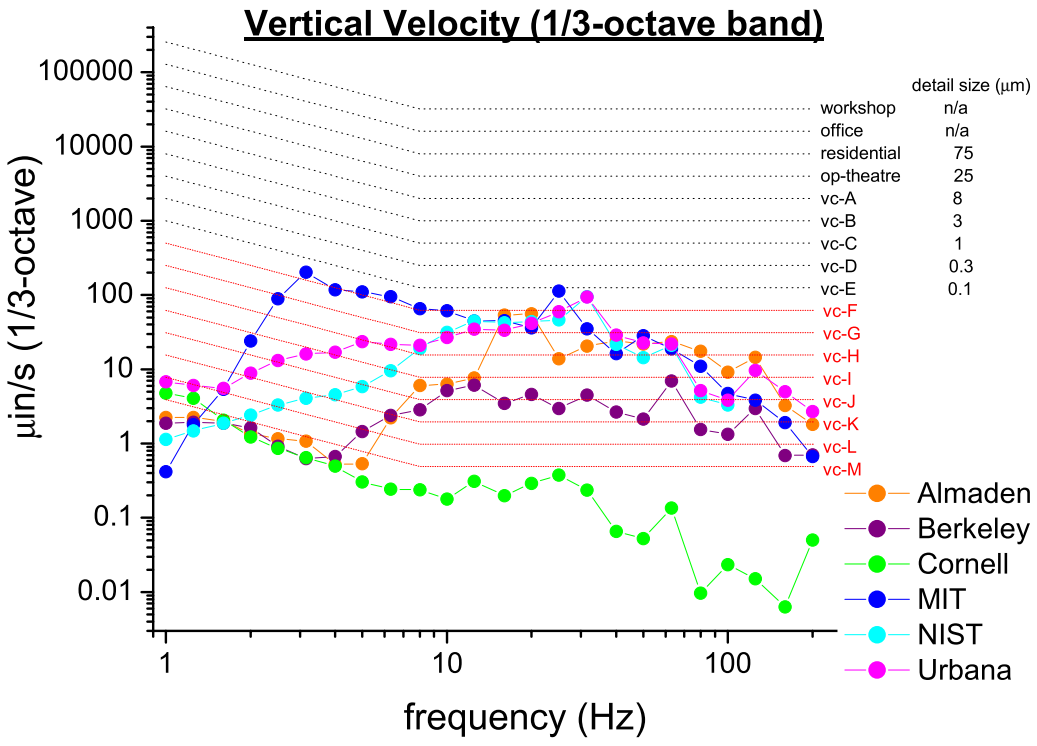

Figure B.10: Vibration measurement results from several STM labs around the country.